Divinyl chlorophyll *a* in the marine eukaryotic protist *Alexandrium ostenfeldii* (Dinophyceae)

Francisco Rodríguez[1*], Anke Kremp[2], José Luis Garrido[3], Cristina Sobrino[4], Geir Johnsen[5], Pilar Riobó[3], José Franco[3], Inga Aamot[5], Isabel Ramilo[1], Noelia Sanz[3]

[1]Instituto Español de Oceanografía (IEO), Centro Oceanográfico de Vigo, Spain.

[2]Marine Research Centre, Finnish Environment Institute, Helsinki, Finland.

[3]Instituto de Investigaciones Marinas (CSIC), Vigo, Spain.

[4]Departamento de Ecología y Biología Animal, Universidad de Vigo, Spain.

[5]Trondhjem Biological Station, Norwegian University of Technology and Science (NTNU), Trondheim, Norway.

[*]For correspondence: e-mail francisco.rodriguez@vi.ieo.es

Key index words: dinoflagellates, *Alexandrium ostenfeldii*, divinyl chlorophyll *a*, pulse amplitude modulated fluorescence, HPLC pigment analysis, LC-MS.

Abbreviations: chl, chlorophyll; chlide, chlorophyllide; DV, divinyl; DVR, 8-vinyl reductase; MV, monovinyl; DV-Pchlide *a*, divinyl protochlorophyllide *a*; PAM, pulse amplitude modulated.

Summary

Here it is reported the first detection of DV-chl *a* together with the usual chl *a* in the marine dinoflagellate *Alexandrium ostenfeldii* from the Baltic Sea. Growth response and photosynthetic parameters were examined at two irradiances (80 and 240 μmol photons $\cdot m^{-2} \cdot s^{-1}$) and temperatures (15º and 19 ºC) in a divinylic strain (AOTV-OS20) *vs* a monovinylic one (AOTV-OS16), using *in vivo* chl *a* fluorescence kinetics of PSII to characterize photosynthetic parameters by pulse amplitude modulated fluorescence, ^{14}C assimilation rates and toxin analyses. The divinylic isolate exhibited slower growth and stronger sensitivity to high irradiance than normal chl *a* strain. DV-chl *a*: chl *a* ratios decreased along time (from 11.3 to <0.5 after 10 months) and to restore them subcloning and selection of strains with highest DV-chl *a* content was required. A mutation and/or epigenetic changes in the expression of divinyl reductase gene/s in *A. ostenfeldii* may explain this altered pigment composition. Despite quite severe limitations (reduced fitness and gradual loss of DV-chl *a* content), the DV-chl *a*-containing line in *A. ostenfeldii* could provide a model organism in photosynthetic studies related with chl biosynthesis and evolution.

Introduction

Chlorophylls are cyclic tetrapyrroles synthesized through a multi-branched pathway (Rebeiz *et al*., 1999; Tanaka and Tanaka, 2007). Chl precursors can accumulate as carrying one vinyl group at C-3 (monovinyl (MV-) pigments) or two vinyl groups at C-3 and C-8 (divinyl (DV-) pigments). In land plants, the 8-vinyl group of DV-chlide *a* is reduced by an 8-vinyl reductase (DVR) enzyme to form the final MV-pigments: chls *a* and *b* (Porra *et al*., 2011)So far, five DVR activities have been detected in the chl biosynthetic pathway (Wang *et al*., 2010). DV chls *a* and *b* in mature cellular plants were first detected in a mutant of *Zea mays* (Bazzaz *et al*., 1982). Recently, DVR genes were identified from chemically-induced *Arabidopsis thaliana* (Nagata *et al*., 2005; Nakanishi *et al*., 2005) and spontaneous DV-mutants (*Oryza sativa*; Wang *et al*. (2010)). Their discovery completed the cluster of genes encoding the pathway for chl biosynthesis in angiosperms (Beale, 2005). However, it cannot be asserted if a single or several DVR enzymes conduct the reduction of the 8-vinyl group of various precursors of chl biosynthesis in other organisms (Nagata *et al*., 2005; Wang *et al*., 2010). To address that issue and to investigate the regulation of these DVR activities DV-mutants are appropriate model organisms (Kolossov *et al*., 2006).

Chl *a* is present in the reaction centers, core and peripheral light-harvesting antennas of almost every oxygenic organism. So far only some marine cyanobacteria are known to replace chl *a* by other chlorophylls in the reaction centers of core complexes: *Prochlorococcus marinus* which contains DV-chl *a* (Chisholm *et al*., 1992) and *Acaryochloris marina* with chl *d* (Kühl *et al*., 2005; Miller *et al*., 2005). The maxima of

absorption in the Soret band (blue region of the visible spectrum) for DV-chl *a* and chl *d* are at considerably longer wavelengths, 442 nm and 452 nm respectively, to that of chl *a* (432 nm; determined in HPLC solvent of Zapata *et al*., 2000; this report and Garrido JL, *pers comm*.). The substitution of chl *a* in these organisms has been associated with an adaptation to maximize light harvesting in specific ecological niches: The cyanobacteria *Acaryochloris marina* grows in biofilms beneath didemnid ascidians, where far-red is enhanced over visible light (Croce and van Amerongen, 2014). Free living forms with chl *d* were also observed in a eutrophic hypersaline lake, a dramatically different environment compared to the relatively pristine waters from which the originally symbiotic forms were isolated (Miller *et al*., 2005). The realized niches of these cyanobacteria were characterized by low availability of dissolved organic C and reduced N as well as a relatively far-red enriched light field. In turn, *Prochlorococcus* is a free-living ubiquitous marine cyanobacteria very abundant in oligotrophic waters where the blue part of the spectrum penetrates the deepest (Partensky *et al*., 1999). It is also characterized by being found in deep layers under stratified conditions (Yacobi *et al*., 1995), with a sharp peak near the bottom of the euphotic zone (Christaki *et al*., 2001). It uses to be concomitant with *Synechococcus* which, in contrast, has chl *a* and dominates the upper layers during stratification periods (Marty and Chiaverini, 2002). The substitution of chl *a* by DV-chl *a*, with absorption in the Soret band (blue region of the visible spectrum) shifted by 8-10 nm to longer wavelengths, could be an evolutionary adaptation in *Prochlorococcus* tailored for collecting photons in oceanic environments.

In the present paper it is reported for the first time the co-occurrence of DV-chl *a* and chl *a* in a eukaryotic microalgae, *Alexandrium ostenfeldii* (Paulsen) Balech & Tangen (Balech and Tangen, 1985), a marine dinoflagellate isolated from the Northern Baltic Sea (Finland). Growth response, photosynthetic parameters and pigment profiles of "divinylic" *A. ostenfeldii* strains were studied, and compared these against the results for "monovinylic" ones (only containing chl *a*). The maintenance of a DV-line required of periodic subcloning because DV-chl *a* decreased significantly after several months in every assayed culture condition. Our results demonstrate that clonal mutants are less tolerant to high irradiances but able to grow with DV-chl *a* harbouring photosystems. The finding of a DV-line of *A. ostenfeldii* represents a potential candidate in photosynthesis research in microalgae to elucidate for example, the DVR enzyme/s, C8-vinyl reduction routes, and the effect of substituting chl *a* by DV-chl *a* in the efficiency of light energy use and the stability of chl-protein complexes.

Results

Pigment analyses and LC-MS characterization of DV-chl a

During a pigment survey on 18 clonal cultures of *Alexandrium ostenfeldii*, isolated from the Northern Baltic Sea (Finland), both chl *a* and DV-chl *a* (molecular structures shown in Fig. 1A) were detected in strains AOTV-B3 and AOTV-C4 in August 2008 (Table 1). All other tested strains only contained chl *a*. Another distinctive feature of AOTV–C4 and AOTV–

B3 relative to the normal pigmented isolates was their lack of chl c_1, although this pigment could be detected in trace amounts in subsequent AOTV-C4 subclones.

Putative DV-chl *a* was isolated and purified from AOTV-OS20 (a DV-strain obtained after 8 subcloning steps from AOTV-C4). The identity of DV-chl *a* was first indicated by HPLC pigment analyses (coelution with authentic DV-chl *a* from the DHI mixed pigments standard in two chromatographic systems; see methods), and comparison with monovinylic strain AOTV-OS16 (chl *a* as dominant pigment with trace amounts of DV-chl *a*, Fig. 1B), and UV-VIS spectral properties (Fig. 1C), and unambiguously identified by LC-MS analyses (Fig. 2). The mass spectrum of the isolated pigment closely resembled that obtained for chl *a*, which in turn matched the general features of published mass spectra (reviewed by Airs and Garrido (2011)). In the DV chl *a* spectrum, all ions appear at m/z values two Daltons (Da) lower, indicating an additional double bond. Sodated (m/z 913.5084) and protonated (m/z 891.5255, consistent with $C_{55}H_{71}MgN_4O_5$, calculated mono-isotopic mass 891.5275 Da, deviation 2.23 ppm) adducts appear in the high masses range (Fig. 2). Main fragment ions result from the formal loss of phytyl (as phytadiene, MH-$C_{20}H_{38}$, $[MH-278]^+$, consistent with $C_{35}H_{33}MgN_4O_5$, calculated monoisotopic mass 613.2301 Da, deviation 3.32 ppm) and from combined losses of phytol and fragments from the methoxycarbonyl substituent at C-13^2 (as formal losses of H_3COH (m/z 581.2029) and $HCOOCH_3$ (m/z 553.2085).

DV-chl a:chl a ratios: temporal evolution and subcloning of divinylic strains

Pigment analyses revealed that DV-chl *a*:chl *a* ratios in AOTV-C4 decreased after some months at levels <1.0 from its initial ratio of 10.99 (Table 1). Therefore, new subclones were periodically isolated from AOTV-C4 in an attempt to select isolates with high DV-chl *a* content, and to explore the variability of DV-chl *a*:chl *a* ratios of its progeny. "1st generation" subclones revealed DV-chl *a*:chl *a* ranging from zero to 1.24. The HPLC results showed that DV-chl *a*:chl *a* ratios were highly variable in 2nd generation subclones, 0.00-1.00 in 27 of them, and 10.27 in AOTV-C4-b28. "3rd generation" subclones from AOTV-C4-b1 (no DV-chl *a*) and AOTV-C4-b28 showed opposite results. DV-chl *a* was not detected in 17 out of 20 subclones from AOTV-C4-b1, and only three exhibited DV-chl *a*:chl *a* ratios of <0.01, 2.80 and 5.59. In turn, all 27 subclones from AOTV-C4-b28 (Fig. 3) showed moderate to high DV-chl *a*:chl *a* (8.42±2.69), close to the initial value (10.27) in the original strain.

Monitoring of DV-chl *a*:chl *a* in AOTV-OS20 revealed a steady decrease from a starting point 11.3 to ~7 after 8 months, and a dramatic reduction until <0.5 in the following 3 months. Once at a minimum DV-chl *a*:chl *a* ratios never recovered again and new subcloning steps were needed to maintain a DV-chl *a* lineage. Subcloning steps allowed maintaining a DV-line until present, but it is noteworthy that establishing DV-strains required bigger efforts since 2014 (due to a reduced growth and lower cellular densities) in comparison with the 2009-2013 period.

Growth rates and photosynthetic performance in DV- vs normal chl a strains

Morphological inspection of DV-strain AOTV-OS20 and normal chl *a* AOTV-OS16 by light microscopy did not show any particular differences in their external appearance, swimming behavior or cell diameter (27.8 ± 4.6 and 28.6 ± 3.9 μm (n=30), in DV- and normal chl *a* strains, respectively).

After 1 month acclimation to experimental conditions batch cultures of the DV-strain showed slower rates of increase for their *in vivo* chl *a* fluorescence than normal chl *a* strain. Maximum fluorescence values (from Turner fluorometer) and final cell densities of DV-strain at 15 ºC (Fig. 4A LL: 4,438 ± 134 cells mL^{-1} and HL: 12,830 ± 1,749 cells mL^{-1}) were significantly lower than normal chl *a* isolate (LL: 39,139 ± 2035 cells mL^{-1} and HL: 31,366 ± 1,686 cells mL^{-1}). Maximum specific growth rates at LL were similar (0.08 d^{-1} and 0.09 d^{-1} for DV- and normal chl *a* strain, respectively), whereas at HL the normal chl *a* isolate doubled its growth rate (0.18 d^{-1}) whereas DV-strain did not (0.08 d^{-1}). In turn, at 19 ºC (Fig. 4B), the differences in final cell densities were smaller among strains and were very similar at the endpoint of each fluorescence curve (2.5-3.5 x 10^3 cells mL^{-1}). At LL normal chl *a* strain grew slightly slower than DV-strain (0.13 d^{-1} and 0.16 d^{-1}, respectively), the contrary being true at HL (0.20 d^{-1} *vs*. 0.15 d^{-1}). The average of *in vivo* chl *a* fluorescence yield per cell was higher in the DV-strain (1.3-3.2 fold, maximum difference observed at 15 ºC, LL), except at 19ºC and HL (0.8).

At the end of the *in vivo* chl *a* fluorescence growth experiment, HL conditions maintained higher DV-chl *a*:chl *a* molar ratios in DV-strain (16.51±0.58 and7.83±1.02 at 15 ºC and 19 ºC, respectively) while low light promoted lower DV-chl *a*:chl *a* (4.62±0.20 and 5.33±0.40 at 15 ºC and 19 ºC, respectively).

Rapid light curves (RLC's) obtained by PAM fluorescence kinetics (Fig. 5) showed a strong reduction in rETR values in DV-strain incubated at HL conditions compared to normal chl *a* strain. Such differences aroused from considerably lower Φ'_{PSII} values between HL acclimated strains (Fig.6). RLC's derived parameters ($\alpha*$, E_k and $rETR_m$) and de-epoxidation state (DES=diatoxanthin/(diadinoxanthin+diatoxanthin)) of the xanthophyll's cycle are summarized in Table 2. At 15 ºC, DV-strain had lower $\alpha*$ (the maximum light utilization coefficient; Sakshaug *et al*. (1997; 1998), lower $rETR_{max}$ (related to P_{max}, the maximum photosynthetic rate), and lower E_k, indicating that non-photochemical quenching (NPQ) started at lower irradiance at this temperature in comparison with normal chl *a* isolate. Extended RLC's (n=17 irradiances) did not vary that much from those shown in Fig. 6, but allowed a better estimate of $\alpha*$ and E_k (Table 2) and strengthened the different responses between normal chl *a* and DV-strain (in this particular case AOTV-OS52, a subclone from AOTV-OS5).

qP and NPQ values were similar in LL acclimated strains. In HL conditions the bad performance of DV-strain precluded comparisons at intensities higher than 476 μmol photons $m^{-2}s^{-1}$. However, at that light step DV-strain acclimated at HL and 15ºC developed much lower qP and NPQ than normal chl *a* strain (Table 2), whereas at 19ºC those trends were not observed.

In HPLC analyses, lower DES values in the normal chl *a* strain *vs* the DV- one were registered in all treatments, especially at 19 ºC and HL, indicating a higher light stress in the DV-strain. It also accumulated a larger pool of Dd resulting in lower peridinin (Per)/Dd

ratios than normal chl *a* strain. Finally, lower chl c_2 ratios normalized to Σ chls *a* (DV-chl *a*+chl *a*) were also found in the DV-strain (2-3 fold times in HL).

RLC's could not be recorded at HL conditions for the whole irradiance range in DV-strain, neither at 15ºC or 19ºC. Despite different dark acclimation times were assayed before running RLC measurements from 10 secs to 15 min (and even >11 hrs in darkness just before the onset of the light cycle), Φ'_{PSII} values laid always <0.3 for DV-strains AOTV-OS20 and AOTV-OS52 in comparison with typical Φ'_{PSII} >0.6 in normal chl *a* strains.

^{14}C assimilation rates

Carbon assimilation normalized by cell number showed similar results as those observed from PAM measurements. Maximum photosynthetic rates and efficiency (P^B_{max} and α, respectively) were higher in normal chl *a* strain (Table 3), and despite the high variability among incubations paired comparisons between results from DV- and normal chl *a* strains resulted in significant differences. E_k was less variable than P^B_{max} and α, and showed lower values in the normal chl *a* strain than in the DV-strain. Photoinhibition at high irradiances was not always observed, but when present, it was higher in the DV-strain (Fig. 7).

LC-MS toxin analyses

PSP toxins profile by UHPLC analyses showed the presence of GTX 2, GTX 3, STX and traces of dcSTX in both DV- and normal chl *a* strains (Table 4). Relative molar proportions were slightly different between isolates: GTX 3 was the dominant toxin in normal chl *a* strain while STX was slightly higher in DV-strain (Table 4). GTX 2 was present in minor

proportions in both strains. On the contrary, same UHPLC analyses were run on a second DV-strain, AOTV-OS5 (obtained from AOTV-OS20 after two subcloning steps), which showed negative results for PSP toxins. Finally, despite SPXs were not detected in any samples, analogues of GYM-A and GYM-B/C were found in the three clones.

Discussion

Growth, toxins and photoacclimation of DV- vs normal chl a strains

Our results reveal that DV-chl *a* producing *A. ostenfeldii* perform less efficiently than the normal chl *a*-containing sibling strains (~40% lower P^{14C}_{m}; Table 3), and lower tolerance to HL (stressed in 15 ºC relative to 19ºC) was evidenced in photosynthetic parameters derived from PAM measurements in DV-strains (e.g.~50% reduction in Φ'_{PSII}, qP and NPQ; Table 2). Photosynthetic performance was always lower in the DV-strain as demonstrated by the direct measurements of organic C assimilation and PAM ETR curves. Lower ability for C fixation without changes in cell volume resulted in the reduction of the growth rates, in agreement with similar findings of photosynthetic rates based on oxygen evolution on a *Synechocystis* DVR mutant (Islam *et al*., 2013).

Slower growth seems directly connected to reduced photosynthetic rates after comparison of PAM results between HL acclimated DV-mutants and only chl *a*-containing strains. This was evidenced by the low Φ'_{PSII} in HL for DV-strain indicating it would need more time to recover from HL damages, the D1 protein of PSII being the most obvious candidate (Valle

et al., 2014), relative to normal chl *a* strain. Intriguingly in our study a recovery of "normal" Φ'_{PSII} values (>0.6) was never observed in HL acclimated DV-strains, because when observed it was concomitant with a major loss of DV-chl *a*.

Previous work on DV-containing organisms, either mutants (Nagata *et al*., 2005; Tomo *et al*., 2009) or *Prochlorococcus* cultures (Moore and Chisholm, 1999), confirm photoinhibition, reduced growth or even cellular death at high light conditions, but the level of photodamage seems to depend on the studied organism (Wang *et al*., 2010).

In previous studies, DV-lines have been found to be less tolerant to high irradiances and this has been explained by the inability of DV-chl *a* to functionally fully substitute chl *a* in the photosynthetic apparatus leading to photo-damage (Nagata *et al*., 2005). The marine cyanobacterium *Prochlorococcus* is also more sensitive to high irradiances and UV radiation than *Synechococcus* (Mella-Flores *et al*., 2012), and Ito and Tanaka (2011), demonstrated that two amino acid residues of the D1 protein are substituted in the photosynthetic reaction center in comparison with the MV-chl-based photosystems. Introducing these substitutions in a *Synechocystis* DVR mutant (which could only survive in LL conditions (Ito *et al*., 2008), led to better light tolerance under medium-light conditions. These studies demonstrated that photodamage in DV-mutants did not occur by abnormal energy dissipation in the antenna system but was caused by the reaction center of PSII. The effects of DV-chl *a* binding to chl-protein complexes were recently studied by chl form analysis in a *Synechocystis* DVR mutant (Islam *et al*., 2013). Blue-shifted chl peaks suggested that, at their binding sites, chls were less stable due to lowered fitting of

the DV-chl *a*, with a consequent destabilization of PSI and PSII complexes. A similar feature could also trigger the reduced tolerance to HL in the DV-strains of *A. ostenfeldii*.

Our results demonstrate that the DV-chl *a* phenotype in *A. ostenfeldii* is less tolerant to high irradiances, but they grow and survive in the long term at these conditions at expenses of a constant loss of DV-chl *a* in favour of chl *a*. Such behavior was possible because DV-lineages always contained chl *a* and after DV-chl *a* decreased to a minimum they recovered a "normal" light tolerance. PAM results and the higher DES of the xanthophylls cycle suggest that DV-strain behaved as a low-light acclimated adapted strain, stressed at HL conditions, in comparison with normal chl *a* strain. However, despite HL acclimated DV-strains yielded noisy PAM measurements and unreliable RLC records, cells still looked healthy under the light microscope.

The gradual loss of DV-chl *a* in *A. ostenfeldii* in the present study probably arises from several factors but a thorough explanation cannot be made clear. Photo-acclimation processes account for changes in the amount and ratios of light-harvesting and photoprotective pigments (Brunet *et al*., 2011). Nevertheless, in our study DV-strains have been maintained in the same culture conditions during several years. Each progeny of DV-strains should be then acclimated to the light and temperature regime and in consequence, the loss of DV-chl *a* would be likely due to other factors. From HPLC pigment results it cannot be concluded if temporal evolution in DV-chl *a*:chl *a* ratios result from either a) the mixture of two cell groups, with or without DV-chl *a*, that progressively become dominated by the second group due to its better overall fitness (growth, photosynthetic efficiency, other), or b) a mixture of DV-chl *a*:chl *a* in each cell that (due to unknown genetic and/or

environmental factors) revert DV-chl *a* into its MV- counterpart. Further physiological, spectroscopic and molecular studies on divinylic *A. ostenfeldii* would benefit from stable DV-chl *a* lineages that, eventually, would not synthesize chl *a* at all. However, to obtain this DV-organism it might be required a transgenic approach, already developed in prokaryotes (Ito and Tanaka, 2011), but still a big challenge in complex eukaryotic cells like dinoflagellates. Notwithstanding, the subcloning approach might not be the best choice to maintain a DV-line in the long term: the reduced fitness of the DV-line in *A. ostenfeldii* since 2014 could be a consequence of such cloning process.

Finally, despite a comprehensive survey on toxin profiles was out of the scope of this work, almost identical results for DV- and normal chl *a* strains indicate that altered pigment composition do not necessarily affect toxins composition or their profile. PSP toxins detected and their relative abundance were those already reported in the literature in *A. ostenfeldii* from the Baltic Sea (Kremp *et al*., 2014). The absence of PSP toxins in DV-strain AOTV-OS5 is not a common feature in *A. ostenfeldii*, but there exist previous reports of non-toxic strains (Kremp *et al*., 2014). Finally, detection of GYM compounds is in agreement with the results obtained for Baltic strains by Salgado *et al*. (2015) and Harju *et al*. (2014).

DV-chl a phenotype – an adaptation to low light conditions?

DV-chls *a* and *b* are considered the exclusive signature of *Prochlorococcus* in the ocean, and it has been suggested that their red-shifted Soret bands relative to MV- chls *a* and *b*

provide an ecological advantage: the superiority to exploit light in the blue part of the spectrum that penetrates deeper layers of oligotrophic waters (Morel *et al*., 1993). In the shallow highly productive coastal waters of the Northern Baltic light penetration is also reduced but its spectrum shifted to longer wavelengths than in the open ocean. Nevertheless, independently of spectral conditions, DV-chl *a* lineages would be competitive in dimly lit layers during the bloom season. Blooms of *A. ostenfeldii* typically occur in the Baltic Sea in late summer at temperatures around and above 20 °C (Hakanen *et al*., 2012). At these temperatures (mimicked by the 19 ºC temperature treatment in our laboratory experiments), and coupled to a low light environment, the DV-chl *a* producing strain had growth rates comparable to the strain that only produced chl *a*. Since the original DV-strains AOTV C4 and AOTV B3 were isolated in summer from a batch that was kept for an extended period of time in dim light, it could be hypothesized that DV-chl *a* production is a response to this condition, i.e. an adaptation to low light environments. Future research should explore into detail the optical properties of the DV-mutants, and the potential effects of other environmental factors, like nutrients, in the pigment profile.

Possible causes for DV-chl a in Alexandrium ostenfeldii

Genetic analyses of multiple *Prochlorococcus* strains (Kettler *et al*., 2007) revealed that, unlike the closely related *Synechococcus* sp. WH8102 (Palenik *et al*., 2003), they lacked homologs of the DVR gene (Dufresne *et al*., 2008). Since the genes neighboring the DVR gene are well conserved in *P. marinus*, this suggests that the ancestor of the genus

Prochlorococcus lost the DVR gene. Thus, absence of chl *a* in *Prochlorococcus* has been explained by a gradual evolutionary substitution of chl *a* by DV-chl *a* or by a mutation/loss of the DVR gene (Nagata *et al*., 2005).

Some chl *a* containing organisms have been shown to also lack the DVR gene (the red alga *Cyanidioschyzon merolae* and the prokaryotes *Synechocystis* sp. PCC6803, *Nostoc* sp. PCC7120, *Thermosynechococcus elongatus* BP-1, *Gloeobacter violaceus* PCC7421 (see refs. in Islam *et al*. (2008), as well as several *Synechococcus* strains (Scanlan *et al*., 2009), supporting the existence of different DVR proteins. In the last years the gene *slr*1923 (also termed *BciB* or *cvrA* sensu Islam *et al.* (2008), in *Synechocystis* sp PCC6803 and *BciA* in the green sulfur bacteria *Chlorobium tepidum*), have been identified to encode alternative 8-vinyl reductases or a modified subunit essential for MV-chl synthesis (Islam *et al*., 2008; Ito *et al*., 2008). In addition, mutant DV-strains of prokaryotic phototrophs, like *Rhodobacter sphaeroides* and *Synechocystis* sp. PCC6803 have been obtained by insertional inactivation or deletion of their native *BciA* or *BciB* genes (Islam *et al*., 2008). However, though homologous DVR genes have been identified in green algae (Nagata *et al*., 2005), the chl biosynthetic pathway and the underlying genes have not yet been fully elucidated in eukaryotic microalgae, and DV-mutants with altered DVR activity have not been found until date.

This report of DV-chl *a* in the dinoflagellate *Alexandrium ostenfeldii* represents the first documentation of this pigment in an eukaryotic microorganism. This might be the result of a mutation in the DVR gene (or genes) leading to an abnormal 8-vinyl reductase activity in the respective strains, as reported for DV-mutants of land plants (Nagata *et al*., 2005; Wang

et al., 2010). Due to the large size and peculiar structure of dinoflagellate genomes, descriptions of genes and gene clusters responsible for biochemical pathways are challenging and sparse compared to other organisms (Jaeckisch *et al*., 2011). Hence, the genetic basis of their Chl *a* synthesis is not fully understood. A DVR gene has not been identified or described in this group of microalgae and the molecular mechanisms behind the observed DV-chl *a* production cannot be directly inferred in contrast with phototrophic prokaryotes (Canniffe *et al*., 2014). Nevertheless, homologs of DVR from land plants and green algae have been found in heterokont algae (Wilhelm *et al*., 2006; Cock *et al*., 2010). Dinoflagellates and heterokont algae have a common ancestor (Janouškovec *et al*., 2010) and apparently share several other genes coding for enzymes of the tetrapyrrole biosynthesis (Koreny *et al*., 2011). This suggests that like heterokonts, also dinoflagellates may contain a plant-type DVR and respective genes.

In contrast to DV-mutants of higher plants that do not synthesize chl *a* at all, or only in trace amounts, DV-strains of *A. ostenfeldii* always contained chl *a*. Moreover, DV-chl *a* was inexorably transformed into chl *a* in contrast to land plants or prokaryotic mutant DV-systems. The selection of progenies with high DV-chl *a*:chl *a* ratios was the only approach to obtain new subclones enriched in DV-chl *a*. The reasons for these fundamental differences between those DV-chl *a* containing organisms might be sought in the unusual genome structure, gene regulation mechanisms and life cycles of dinoflagellates (Jaeckish *et al*., 2011). For instance, recent transcriptome sequencing of different *Alexandrium* species revealed the presence of multiple copies for many genes, for example saxitoxin genes (Stüken et al., 2011; Orr et al., 2013), or the peridinin complex protein (PCP) gene in

A. ostenfeldii (Jaeckisch *et al*., 2011). Different copies of the DVR gene could also coexist in this organism.

Alternative to mutation, epigenetic phenomena could be responsible for the coexistence of DV-chl *a* and chl *a* in *A. ostenfeldii* and explain unstable DV-chl *a*:chl *a* ratios. Epigenetic effects seem to be widespread from protists to humans (Tollefsbol, 2011). They affect the gene transcription without associated changes in the DNA sequence and ultimately determine which genes are expressed and which not. For instance, epigenetic regulation has been suggested as a possible mechanism to explain the complex mating system and intraclonal variability of cyst production and progeny viability in the dinoflagellate *Gymnodinium catenatum* (Figueroa *et al*., 2010). Epigenetics involve the regulation of gene expression through mechanisms like the introduction of unusual histone proteins, altered chromatin structures, DNA methylation, non-coding RNA's, etc (Cheng *et al*., 2011) which may all alter the functionality of the genes. So far, the regulation of gene expression through epigenetic mechanisms is completely unknown in dinoflagellates.

Another characteristic feature in DV-chl *a* containing *A. ostenfeldii* was the lack of chl c_1 in the original pigment analyses of AOTV-C4 and AOTV-B3 strains. Chl c_1 is the monovinylic analogue of chl c_2 (Zapata *et al*., 2006), the latter being its precursor in the proposed biosynthetic route of *c*-type chls (Porra *et al*., 2011). Therefore, the lack (or trace levels) of chl c_1 could be associated with the fault in the same DVR activity (or its low expression) that leads to accumulate DV-chl *a*. Some "normal pigmented" strains already contained very low amounts of Chl c_1 (AOTV-A1 and A4, Table 1), and that observation could help to explain why a DV-strain with very low DV-chl *a*:chl *a* ratios like AOTV-B3

(Table 1) lacked also chl c_1. In fact, it has been recently shown that DVR from *Synechocystis* (*Slr1923*), a ferredoxin-dependent DVR like one of the two DVR's reported in diatoms, converts efficiently chl c_2 into chl c_1 (Ito and Tanaka, 2014). In addition, replacement of chl *a* by DV-chl *a* in DV-strains of *A. ostenfeldii* could induce some alteration in the size or composition of light-harvesting antennae as evidenced by the reduced chl *c* content relative to normal chl *a* strains.

Compared to land plants, the knowledge on DVR activity and its regulation in microalgae is very limited. For example, it is not understood how isolates of the cyanobacterium *Prochlorococcus* lacking a DVR enzyme are able to transform DV-chl *b* into chl *b* under HL conditions (Partensky *et al.*, 1999). The exact mechanisms underlying the possible transformation of DV-chl *a* to chl *a* in *A. ostenfeldii* remain the object of future studies. Such would, however, have a high potential to elucidate fundamental processes in the chl *a* synthesis pathway of dinoflagellates and eukaryotic microorganisms in general.

Conclusions

This study, for the first time, reports DV-chl *a* in a eukaryotic microorganism. The co-existence of DV-chl *a* and chl *a* in cultured *A. ostenfeldii* could make this species a potential new model organism for further genetic and/or epigenetic studies to better understand the tetrapyrrole biosynthetic pathway, the regulation of 8-vinyl reduction of DV-chls in oxygenic photoautotrophs, as well as the possible replacement of chl *a* by DV-chl *a* in the reaction centers. Ideally, the instability of DV-chl *a* in mutants would need to

be overcome, first to prevent the irreversible loss of this pigment, and to facilitate further research on stable model organisms. But such stability could be compromised if a epigenetic regulation of the DV-phenotype is demonstrated. Some fundamental issues as, for example, if several enzymes or a single one with broad specificity conducts the reduction of the 8-vinyl group in chl biosynthesis, could be addressed using the DV-phenotype. Our report also anticipates the possibility to detect DV-chl *a* in natural samples from other microalgae than *Prochlorococcus*, challenging its traditional role as specific marker pigment to trace populations of *Prochlorococcus* in the world's oceans (Bouman *et al*., 2006).

Experimental procedures

Culture conditions

Alexandrium ostenfeldii strains studied (Table 1) were established from single cells isolated in 2004 (AOTV-A1, AOTV-A4, AOTV-B3 and AOTV-C4) and 2008 (AOTV-0801 to AOTV-0816), respectively, from bloom samples collected in Överö Sound/Föglö in the Åland archipelago, at the northern end of the Baltic Proper off the SW coast of Finland (Kremp *et al*., 2009). The sample from the 2004 bloom was left standing under a shelf at dim light conditions for approximately 10 months before cells were isolated and brought into culture. Cultures were maintained in 50 mL glass flasks and L1 medium without silicates (Guillard and Hargraves, 1993) made with seawater from Ría de Vigo. Salinity was adjusted to 10 psu as strains were originally isolated from the low saline (salinity of 6-

7) Baltic Sea. All strains were initially incubated at 19 ºC and an irradiance (E) of 90 µmol photons · $m^{-2} \cdot s^{-1}$ (E_{PAR}, Photosynthetically Active Radiation at 400-700 nm), measured with a QSL-100 irradiance meter (Biospherical Instruments Inc. San Diego, CA, USA) and at a 12:12 L:D photoperiod. Experimental setups included two distinct temperatures (15 ºC and 19 ºC), low light acclimated cells (LL) grown at E of 80 µmol photons ·$m^{-2} \cdot s^{-1}$and high light acclimated cells (HL) grown at E of 240 µmol photons ·$m^{-2} \cdot s^{-1}$. Cells were acclimated for at least two generations to each experimental combination of temperature and light. Culture growth was monitored by *in vivo* chl *a* fluorescence using a Turner designs 10-AU fluorometer. Specific growth rates were calculated from fluorometer results as $\mu = ((\ln [F_2] - \ln [F_1]) / (t_2 - t_1))$ (1), where *F* denotes *in vivo* chl *a* fluorescence recorded at time *t* (days).

Subcloning A. ostenfeldii

As DV-chl *a* progressively decreased in AOTV-C4 cultures, single cells were isolated with a capillary micropipette to screen for subclones with high DV-chl*a*:chl *a* ratios. Single cell isolates were grown in 96-multiwell plates with L1 medium adjusted to salinity of 10, at 19 ºC. The subclones that developed into new cultures needed 1-2 months before cell numbers increased enough to perform HPLC pigment analyses. At each subcloning step, the strain with highest DV-chl *a*:chl *a* ratios served as a source for isolating new subclones, to maintain the lineage of "divinylic" *A. ostenfeldii*. "1st Generation" clones were labelled as AOTV-C4-a#(n=12), "2nd generation" subclones (from AOTV-C4-a5) as AOTV-C4-b#

(n=28), and "3rd generation" subclones (from AOTV-C4-b1 (n=20) and AOTV-C4-b28 (n=27)), were not labelled individually. Amongst the subclones derived from AOTV-C4-b28, a 3rd generation isolate with DV-chl *a*:chl *a* = 7.6 continued the subcloning steps. In overall, 19 subcloning rounds have been performed during 60 months (January 2010-2015). This procedure enabled us to maintain a lineage of high DV-chl *a* until present, excepting a period of low DV-chl *a*:chl *a* between the 4th-7th generations. To follow the trend of DV-chl *a*:chl *a* over time in an individual subclone the pigment profile in strain AOTV-OS20 (obtained after 8 subcloning steps from AOTV-C4), was periodically analysed during 10 months (see results section). Another subclone, AOTV-OS16, obtained at the same subcloning step than AOTV-OS20 showed trace levels of DV-chl *a* and was used to compare their growth and photosynthetic performance of both subclones.

Pigment analyses

Cells were harvested 3 h into the light cycle from cultures in exponential growth phase. 10-20 mL of cultures were filtered onto Whatman GF/F filters (nominal pore size 0.7 μm, Whatman International Ltd., UK), under low pressure to avoid damage of the cells. In addition, a serial filtration through Whatman GF/D (nominal pore size 2.7 μm) and GF/F filters was performed to discard any source of contamination from picoplankton cells for DV-Chl *a* detected in AOTV-C4. Filters were frozen and kept at -20ºC until further analysis. Pigment extracts were done under low light in Teflon-lined screw capped tubes with 5 mL 90% acetone using a stainless steel spatula for filter grinding. The tubes were

chilled in a beaker of ice and sonicated for 5 min in an ultrasonic bath (Raypa Espinar, S.L., Terrassa, Spain). Extracts were then filtered through 13 mm diameter syringe filters (MSPTFE, 0.22 μm pore size, hydrophilic PTFE, Membrane Solutions, Plano, Texas) to remove cell and filter debris. In order to avoid peak distortion, which affects early eluting pigments, 0.4 mL of milli-Q (Millipore, Bedford, MA, USA) water was added to each mL of acetone extract immediately before injection (Zapata and Garrido, 1991). Pigments were separated using a Waters (Waters Corporation, Milford, MA) Alliance HPLC System consisting of a 2695 separations module, a Waters 996 diode-array detector and a Waters 474 scanning fluorescence detector. Pigment separation was performed following Zapata *et al*. (2000), modified as described below. The column was a C8 Waters Symmetry (150x4.6 mm, 3.5 μm particle-size, 100 Å pore-size). Eluent A was methanol:acetonitrile:0.025 M aqueous solution of pyridine (50:25:25, v/v/v). Eluent B was methanol:acetonitrile:acetone (20:60:20 v/v/v). Elution gradient was: (time: %B) 0 min: 0%, 22 min:40%, 28 min: 95%, 37 min: 95%, 40 min: 0%. Flow rate was 1.0 mL min^{-1} and column temperature was 25 ºC. Pigments were identified either by co-chromatography with authentic standards obtained from SCOR reference cultures, the mixed phytoplankton pigments standard from DHI (Hoersholm, Denmark) and diode-array spectroscopy. For identification purposes selected samples containing the putative DV-chl *a* were analysed in a second chromatographic system (Garrido and Zapata, 1997). After checking for peak purity, spectral information was compared with a library of chl and carotenoid spectra from pigments prepared from standard phytoplankton cultures (SCOR cultures, Roy *et al*. (2011)). External calibration with pigment standards isolated in our laboratory (quantified by VIS spectroscopy using

their corresponding extinction coefficients provided in Egeland *et al*., (2011)), were used to derive quantitative data from chromatograms at 440 nm (1.2 nm band width). A rapid exam of DV-chl *a* to chl *a* ratios was done comparing the areas of both peaks in chromatograms extracted at 664.5 nm, corrected with the corresponding recommended extinction coefficients.

LC-MS analyses of DV-chl a

High resolution positive ion mass spectra of chl *a* and 8-[vinyl]-chl *a* were obtained with a Thermo Scientific Dionex Ultimate 3000 High-Speed LC (column: Acquity HSS C18, 1.8 µm, 150 x 2.1 mm; isocratic elution with 0.1 % formic acid in methanol:water 9:1, flow rate 200 µL min^{-1}) coupled to an Exactive mass spectrometer, equipped with an Orbitrap mass analyzer and a HESI-II probe for electrospray ionization. Full scan and AIF (all ion fragmentation) scans were acquired. Mass calibration was performed with a mixture consisting of caffeine, MRFA tetrapeptide, and Ultramark 1621. All analyses were performed using the "balanced" automatic gain control (AGC) setting with a 200 ms maximum inject time. Data acquisition was carried out using ThermoScientific Xcalibur 2.1. Optimal ion source and interface conditions consisted of a spray voltage of 4 kV, sheath gas flow of 25, auxiliary gas flow of 7, capillary temperature of 320 ºC, in-source collision induced dissociation (CID) of 0.0 eV and normalized collision energy (NCE) of 35%. For Full MS spectra conditions were as follows: Microscans 1; Resolution 70,000; AGC target 3e6; Maximum IT 200 ms; Scan range 120 to 1200 m/z. In AIF mode:

Microscans 1; Resolution 35,000; AGC target 3e6; Maximum IT 100 ms; NCE (normalized collision energy) 35.0; Scan range 120 to 1000 *m/z*.

In vivo PSII fluorescence measurements

Photosynthetic parameters, based on electron transfer rate (ETR) data, were estimated with a Phyto-PAM (Heinz Walz GmbH, Effeltrich, Germany). Photosynthetic and bio-optical parameters used in this study are listed in Table 5 and were defined according to (Sakshaug *et al*., 1997; Sakshaug *et al*., 1998). PAM measurements were performed on cells in exponential growth phase. Samples were placed in a quartz cuvette equipped with a magnetic stirrer. Rapid light curve (RLC) measurements followed the "quasi-darkness" approach proposed by Ralph and Gademann (2005) to compare the current light acclimation state of DV-strains *vs* normal chl *a* ones in each treatment (light and temperature). The "quasi-darkness" approach consists in a short dark acclimation (10 seconds) prior to RLC measurements, that allows the rapid re-oxidation of primary electron acceptor (Q_A), but not a significant relaxation of the non-photochemical quenching (NPQ) coefficient (Schreiber, 2004). In these conditions it is obtained an operational quantum yield in actinic light (Φ'_{PSII}; mol electrons · [mol quanta]$^{-1}$), calculated as $\Phi'_{PSII} = F'_v - F'_0/F'_m$ (2) where F'_v is the variable fluorescence defined as $F'_m - F'_0$, the maximum and minimum PSII fluorescence yield, respectively (measured on light-acclimated cells). Longer dark acclimation periods (up to 15 min) were also assayed but HL acclimated DV-strains did not show significantly different Φ'_{PSII} values (<0.3 in all cases) to those samples acclimated for

10 s to dark conditions. Photochemical quenching (qP) and NPQ were calculated by WinControl software v2.08 with the equations: qP = (F_m'-F)/(F_m'-F_0') (2), NPQ =(F_m-F_m')/F_m' (3), (Brunet *et al*., 2011), where F is the fluorescence yield measured briefly before application of the last saturation pulse (in the presence of actinic light). F_m is the maximal fluorescence yield of a dark-acclimated sample, but in our case it should be quoted as F_m' because samples were not fully dark-acclimated before RLC analyses.

RLC's were performed in triplicate, 4-6 h after the onset of the light period, by applying 8 increasing actinic irradiances from 100 to 1700 µmol photons · m^{-2} · s^{-1} (60 to 1100 for divinylic strains), 30 s width (illumination exposure) at each light level. For comparison purposes, RLC's were also assayed in an extended fashion to 17 irradiances. However, due to software limitations, this approach required of two different measurements on the same culture (RLC1 and RLC2, with 5 min of dark adaptation before each RLC, and 1 min width at each light level, from 7 to 1500 µmol photons · m^{-2} · s^{-1}). To quantitatively compare RLC's, relative electron transport rates (rETR= Φ'_{PSII} x E_{PAR} x 0.5, (4); Genty *et al*. (1989)) averaged RLC values were fitted into Sigmaplot v10.0 (Systat Software, Inc., Chicago, IL, USA), using the model of Webb *et al.* (1974), according to the following equation:

$$\mathbf{rETR} = \mathbf{rETR}_{\max}\left[1-\exp\left(-\alpha^{*}\cdot\frac{\mathbf{E_{PAR}}}{\mathbf{rETR_{max}}}\right)\right]$$ (6) where $\alpha*$ is the maximum light utilization coefficient ($\alpha^{*} = \frac{\mathbf{rETR_m}}{E_k}$), $rETR_m$ is the maximum relative electron transport rate, and E_k is the light saturation index (µmol photons · m^{-2} · s^{-1}).

^{14}C assimilation rates

Photosynthetic response of DV-strain (AOTV-OS20) and normal chl *a* strain (AOTV-OS16) to PAR irradiance was also measured as the uptake of $H^{14}CO_3^-$ (approximately 0.5 μCi mL^{-1}) into organic compounds during 1 h incubation period in a photosynthetron incubator (CHPT Manufacturing Inc., Delaware, USA). For the ^{14}C incubations, cultures were previously acclimated at 19ºC and 240 μmol photons · m^{-2} · s^{-1}. Samples from each strain (1 mL) were incubated at 19 ºC in 7 mL scintillation vials exposed to 24 different irradiances that were obtained by filtering irradiance from a 250W halogen lamp with neutral density screens. Irradiance was measured with a quantum scalar sensor (QSL-100) mounted inside a scintillation vial. Incubation of both strains was performed simultaneously at three different times within a 5 months time period (n=3). HCl was used to terminate photosynthesis (0.25 mL of 1.2 N HCl to each cuvette), and to ensure the removement of all inorganic CO_2. The vials were shaken overnight after which scintillation cocktail was added and incorporated ^{14}C was measured in a liquid scintillation analyzer (WALLAC 1409-012). Total DIC was determined with a LI-7000 CO_2 Gas analyzer (Li-Cor Inc.). Photosynthetic parameters P_m^{14C} and E_k, were estimated as for the PAM data, by fitting the values to the equation from (Jassby and Platt, 1976): $$P^{14C} = P_m^{14C} \tanh\left(\alpha^{14C} \cdot \frac{E_{PAR}}{P_m^{14C}}\right) \quad (7),$$ where P^{14C} is the photosynthetic rate per unit of chl biomass (mg C [mg Chl *a*]$^{-1}$ h^{-1}), and P_m^{14C} the maximum photosynthetic rate normalized to chl biomass (same as above).

Toxin analyses: analyses of PSP toxins.

PSP toxins were analyzed by high-performance liquid chromatography (HPLC) with post-column oxidation and fluorescence detection (FD) according to the method of Rourke *et al.* (2008), with slight modifications. The analyses were carried out using a Waters Acquity ultra performance liquid chromatography (UPLC) system (Waters, USA). The toxins were separated on a Zorbax Bonus RP column (4.6 × 150 mm, 3.5 μm). Mobile phase A was composed of 11 mM heptane sulfonic acid sodium salt in a 5.5 mM phosphoric acid aqueous solution adjusted to pH 7.1 with 0.5 M ammonium hydroxide. Mobile phase B consisted of 88.5% 11 mM heptane sulfonic acid sodium salt in a 16.5 mM phosphoric acid aqueous solution adjusted to pH 7.1 with 0.5 M ammonium hydroxide and 11.5% acetonitrile. The mobile phases were filtered through a 0.2 μm Nylon pore size, 47 mm diameter membrane filter (Whatman) before use. A gradient was run at a flow rate of 0.8 mL min^{-1} starting at 100% A and held for 8 min. Mobile phase B was then increased linearly to 100% in 8 min. The gradient was kept at 100% B for 9 min and then returned in 0.1 min to 100% A. An equilibration time of 5 min was allowed prior to the next injection. The total duration of the run was 30 min. The eluate from the column was mixed continuously with 7 mM periodic acid in 50 mM potassium phosphate buffer (pH 9.0) at a rate of 0.4 mL min^{-1} and was heated at 65 °C by passage through a coil of Teflon tubing (0.25 mm i.d., 8 m long). It was then mixed with 0.5 M acetic acid at 0.4 mL min^{-1} and pumped by a two-pump Waters Reagent Manager into the fluorescence detector, which was operated at an excitation wavelength of 330 nm, recording emission at 390 nm. Data acquisition and data processing were performed using the Empower data system (Waters).

Toxin concentrations were calculated from calibration curves obtained for the peak area and amount of each toxin. Injection volumes of 20 μL were used for each extract. Standards for the PSP toxins gonyautoxin (GTX)-4, GTX-1, dcGTX-3, dcGTX-2, GTX-3, GTX-2, neoSTX, dcSTX, and STX were acquired from the NRC certified reference material program (Halifax, NS, Canada). To verify the presence of, GTX-6 and GTX-5, the samples were boiled with an equal volume of 0.4 M HCl for 15 min to hydrolyze the sulfonic group of the N-sulfocarbamoyl, yielding the corresponding carbamoyl toxins (Franco and Fernández-Vila, 1993).

Analyses of lipophilic toxins (SPXs and GYMs)

SPX and GYM toxins were identified by liquid chromatography coupled to high-resolution mass spectrometry (LC–HRMS). Samples in methanol were analyzed on a Dionex Ultimate 3000 LC system (Thermo Fisher Scientific, San Jose, California) coupled to an Exactive mass spectrometer (Thermo Fisher Scientific, Bremen, Germany) equipped with an Orbitrap mass analyzer and a heated electrospray source (H–ESI II). Nitrogen (purity > 99.999%) was used as the sheath gas, auxiliary gas, and collision gas. The instrument was calibrated daily in positive and negative ion modes. Mass acquisition was performed in positive ion mode without and with an all ion fragmentation (AIF) HCD 45 eV. The mass range was *m/z* 100–1000 in both full-scan and AIF modes.

SPXs and GYMs were separated and quantified according to the Standardized Operating Procedure (SOP) validated by the European Union Reference Laboratory for Marine

Biotoxins (EURLMB, 2011). The X-Bridge C18 column (100 × 2.1 mm, 2.5 μm) was maintained at 25 °C; the injection volume was 20 μL and the flow rate 400 μL min^{-1}. Mobile phase A consisted of water, and mobile phase B of acetonitrile/water (95:5 v/v), both containing 2 mM ammonium formate and 50 mM formic acid. Linear gradient elution started at 10% B, increasing to 80% B in 4 min, where it was held for 2 min before the initial conditions of 10% B were restored in 0.5 min; the latter condition was maintained for 2.5 min to allow column equilibration. The total duration of the run was 9 min. Several SPX toxins were screened including 13dMeC, 20MeG, A, B, C, D, desmethyl SPX-D, and the unknown SPXs listed by Sleno *et al*., (2004). Cyclic imines standards for SPX-1 (13-desmethyl SPX-C; CRM-SPX-1 7.06 ± 0.4 μg mL^{-1}) and GYM-A (CRM-GYM-A 5 ± 0.2 μg mL^{-1}) were acquired from the NRC Certified Reference Material (CRM) Program.

Statistical analysis

Significant differences between DV- and normal chl *a* strains were tested using a paired Student *t*-test using SigmaPlot (Systat Software, San Jose, CA). *P* values <0.005 were considered significant.

Acknowledgments

This work is a contribution of "Microalgas Nocivas, (IEO), Unidad Asociada al IIM (CSIC), and was carried out at the Instituto Español de Oceanografía (IEO) in Vigo. We

thank H. Scheer, S. Roy, C. Six and G. Alvarez for critical reading earlier versions of this manuscript. This work was partially funded by the culture collection of harmful microalgae of IEO (CCVIEO). J.L.G. acknowledges financial support from Xunta de Galicia (project PGIDT02RMA40202PR). Funding was also provided by the Academy of Finland (grant # 128833 to A.K.). We wish also to dedicate this work to our colleague and friend M. Zapata who contributed in the first versions of this manuscript. All authors disclose any potential sources of conflict of interest.

References

Airs, R.L., and Garrido, J.L. (2011) Liquid chromatography-mass spectrometry for pigment analysis. In *Phytoplankton pigments: characterization, chemotaxonomy, and applications in oceanography*. Roy, S., Llewellyn, C.A., Egeland, E.S., and Johnsen, G. (eds). New York: Cambridge University Press, pp. 314-342.

Balech, E., and Tangen, K. (1985) Morphology and taxonomy of toxic species in the tamarensis group (Dinophyceae): *Alexandrium excavatum* (Baarud) comb. nov. and *Alexandrium ostenfeldii* (Paulsen) comb. nov. *Sarsia* **70**: 333-343.

Bazzaz, M.B., Bradley, C.V., and Brereton, R.G. (1982) 4-vinyl-4-desethyl chlorophyll *a*: characterisation of a new naturally occurring chlorophyll using fast atom bombardment, field desorption and "in beam" electron impact mass spectroscopy. *Tetrahedron Lett* **23**: 1211-1214.

Beale, S.I. (2005) Green genes gleaned. *Trends Plant Sci* **10**: 309-312.

Bouman, H., Ulloa, O., Scanlan, D., Zwirglmaier, K., Li, W., Platt, T. et al. (2006) Oceanographic basis of the global distribution of *Prochlorococcus* ecotypes. *Science* **312**: 918-921.

Brunet, C., Johnsen, G., Lavaud, J., and Roy, S. (2011) Pigments and photoacclimation processes. In *Phytoplankton pigments: characterization, chemotaxonomy, and applications in oceanography*. Roy, S., Llewellyn, C.A., Egeland, E.S., and Johnsen, G. (eds). New York: Cambridge University Press, pp. 445-471.

Canniffe, D.P., Chidgey, J.W., and Hunter, C.N. (2014) Elucidation of the preferred routes of C8-vinyl reduction in chlorophyll and bacteriochlorophyll biosynthesis. *Biochem J* **462**: 433-440.

Cheng, X., Hashimoto, H., Horton, J., and Zhang, X. (2011) Mechanisms of DNA Methylation, Methyl-CpG recognition, and Demethylation in Mammals. In *Handbook of epigenetics: the new molecular and medical genetics*. Tollefsbol, T. (ed). USA: Academic Press, Elsevier, pp. 9-24.

Chisholm, S.W., Frankel, S.L., Goericke, R., Olson, R.J., Palenik, B., Waterbury, J.B. et al. (1992) *Prochlorococcus marinus* nov. gen. nov. sp.: an oxyphototrophic marine prokaryote containing divinyl chlorophyll *a* and *b*. *Arch Microbiol* **157**: 297-300.

Christaki, U., Courties, C., Karayanni, H., Giannakourou, A., Maravelias, C., Kormas, K.A., and Lebaron, P. (2001) Dynamic characteristics of *Prochlorococcus* and *Synechococcus* consumption by bacterivorous nanoflagellates. *Microb Ecol* **43**: 341-352.

Cock, J., Sterck, L., Rouzé, P., Scornet, D., Allen, A., Amoutzias, G. et al. (2010) The *Ectocarpus* genome and the independent evolution of multicellularity in brown algae. *Nature* **465**: 617-621.

Croce, R., and van Amerongen, H. (2014) Natural strategies for photosynthetic light harvesting. *Nat Chem Biol* **10**: 492-501.

Dufresne, A., Ostrowski, M., Scanlan, D., Garczarek, L., Mazard, S., Palenik, B. et al. (2008) Unraveling the genomic mosaic of a ubiquitous genus of marine cyanobacteria. *Genome Biol* **9**: R90.

Egeland, E.S., Garrido, J.L., Clementson, L., Andresen, K., Thomas, C.S., Zapata, M. et al. (2011) Data sheets aiding identification of phytoplankton carotenoids and chlorophylls. In *Phytoplankton pigments: characterization, chemotaxonomy, and applications in oceanography*. Roy, S., Llewellyn, C.A., Egeland, E.S., and Johnsen, G. (eds). New York: Cambridge University Press, pp. 665-822.

EURLMB (2011). EU-Harmonised Standard Operating Procedure for Determination of Lipophilic Marine Biotoxins in Molluscs by LC–MS/MS. European Union Reference Laboratory for Marine Biotoxins. http://aesan.msps.es/en/CRLMB/web/home.shtml.

Figueroa, R., Rengefors, K., Bravo, I., and Bensch, S. (2010) From homothally to heterothally: Mating preferences and genetic variation within clones of the dinoflagellate *Gymnodinium catenatum*. *Deep-Sea Res Pt II* **57**: 190–198.

Franco, J., and Fernández-Vila, P. (1993) Separation of Paralytic Shellfish Toxins by Reversed Phase High Performance Liquid Chromatography, with Postcolumn Reaction and Fluorimetric Detection. *Chromatographia* **35**: 613-620.

Garrido, J.L., and Zapata, M. (1997) Reversed-phase high-performance liquid chromatography of mono- and divinyl chlorophyll forms using pyridine-containing mobile phases and polymeric octadecylsilica. *Chromatographia* **44**: 43-49.

Genty, B., Briantais, J.M., and Baker, N.R. (1989) The relationship between the quantum yield of photosynthetic electron transport and quenching of chlorophyll fluorescence. *Biochim Biophys Acta* **990**: 87–92.

Guillard, R.R.L., and Hargraves, P.E. (1993) *Stichochrysis immobilis* is a diatom, not a chrysophyte. *Phycologia* **32**: 234-236.

Hakanen, P., Suikkanen, S., Franzén, J., Franzén, H., Kankaanpää, H., and Kremp, A. (2012) Bloom and toxin dynamics of *Alexandrium ostenfeldii* in a shallow embayment at the SW coast of Finland, Northern Baltic Sea. *Harmful Algae* **15**: 91-99.

Harju, K., Kremp, A., Suikkanen, S., Kankaanpää, H., and Vanninen, P. (2014) Mass spectrometric screening of novel gymnodimine-like compounds in isolates of *Alexandrium ostenfeldii*. In. 16th International Conference on Harmful Algae, Wellington, New Zealand.

Islam, M.R., Aikawa, S., Midorikawa, T., Kashino, Y., Satoh, K., and Koike, H. (2008) slr1923 of Synechocystis sp. PCC6803 is essential for conversion of 3,8-Divinyl(proto)chlorophyll(ide) to 3-Monovinyl(proto)chlorophyll(ide). *Plant Physiol* **148**: 1068-1081.

Islam, R., Watanabe, K., Kashino, Y., Satoh, K., and Koike, H. (2013) Spectral properties of a divinyl chlorophyll *a* harboring mutant of *Synechococcus*. *Photosynth Res* **117**: 245-255.

Ito, H., and Tanaka, A. (2011) Evolution of a divinyl chlorophyll-based photosystem in *Prochlorococcus*. *P Natl Acad Sci USA* **108**: 18014-18019.

Ito, H., and Tanaka, A. (2014) Evolution of a new chlorophyll metabolic pathway driven by the dynamic changes in enzyme promiscuous activity. *Plant Cell Physiol* **55**: 593-603.

Ito, H., Yokono, M., Tanaka, R., and Tanaka, A. (2008) Identification of a novel vinyl reductase gene essential for the biosynthesis of monovinyl chlorophyll in *Synechocystis* sp. PCC6803. *J Biol Chem* **283**: 9002-9011.

Jaeckisch, N., Yang, I., Wohlrab, S., Glöckner, G., and Kroymann, J. (2011) Comparative genomic and transcriptomic characterization of the toxigenic marine dinoflagellate *Alexandrium ostenfeldii*. *PLoS One* **6**: e28012.

Janouškovec, J., Horák, A., Oborník, M., Lukeš, J., and Keeling, P.J. (2010) A common red algal origin of the apicomplexan, dinoflagellate, and heterokont plastids. *P Natl Acad Sci USA* **107**: 10949-10954.

Jassby, A.D., and Platt, T. (1976) Mathematical formulation of the relationship between photosynthesis and light for phytoplankton. *Limnol Oceanogr* **21**: 540-547.

Kettler, G.C., Martiny, A.C., Huang, K., Zucker, J., Coleman, M.L., Rodrigue, S. et al. (2007) Patterns and implications of gene gain and loss in the evolution of *Prochlorococcus*. *PLoS Genet* **3**: e231.

Kolossov, V.L., Bohnert, H.J., and Rebeiz, C.A. (2006) Chloroplast biogenesis 92: In situ screening for divinyl chlorophyll(ide) alpha reductase mutants by spectrofluorometry. *Anal Biochem* **348**: 192-197.

Koreny, L., Sobotka, R., Janouškovec, J., Keeling, P., and Oborník, M. (2011) Tetrapyrrole synthesis of photosynthetic chromerids is likely homologous to the unusual pathway of apicomplexan parasites. *Plant Cell* **23**: 3454-3462.

Kremp, A., Lindholm, T., Dreßler, N., Erler, K., Gerdts, G., Eirtovaara, S., and Leskinen, E. (2009) Bloom forming *Alexandrium ostenfeldii* (Dinophyceae) in shallow waters of the Åland Archipelago, Northern Baltic Sea. *Harmful Algae* **8**: 318-328.

Kremp, A., Tahvanainen, P., Litaker, W., Krock, B., Suikkanen, S., Leaw, C., and Tomas, C. (2014) Phylogenetic relationships, morphological variation and toxin patterns in the *Alexandrium ostenfeldii* (Dinophyceae) complex: implications for species boundaries and identities. *J Phycol* **50**: 81-100.

Kühl, M., Chen, M., Ralph, P., Schreiber, U., and Larkum, A. (2005) A niche for cyanobacteria containing chlorophyll *d*. *Nature* **433**: 820.

Marty, J.C., and Chiaverini, J. (2002) Seasonal and interannual variations in phytoplankton production at DYFAMED time-series station, northwestern Mediterranean Sea. *Deep-Sea Res Pt II* **49**: 2017-2030.

Mella-Flores, D., Six, C., Ratin, M., Partensky, F., Boutte, C., Le Corguillé, G. et al. (2012) *Prochlorococcus* and *Synechococcus* have evolved different adaptive mechanisms to cope with light and UV stress. *Front Microbiol* **3**: 285.

Miller, S.R., Augustine, S., Olson, T.L., Blankenship, R.E., Selker, J., and Wood, A.M. (2005) Discovery of a free-living chlorophyll d-producing cyanobacterium with a hybrid proteobacterial/cyanobacterial small-subunit rRNA gene. *P Natl Acad Sci USA* **102**: 850-855.

Moore, L.R., and Chisholm, S.W. (1999) Photophysiology of the marine cyanobacterium *Prochlorococcus*: ecotypic differences among cultured isolates. *Limnol Oceanogr* **44**: 628-638.

Morel, A., Ahn, Y.-W., Partensky, F., Vaulot, D., and Claustre, H. (1993) *Prochlorococcus* and *Synechococcus*: a comparative study of their size, pigmentationand related optical properties. *J Marine Syst* **51**: 617-649.

Nagata, N., Tanaka, R., Satoh, S., and Tanaka, A. (2005) Identification of a vinyl reductase gene for chlorophyll synthesis in *Arabidopsis thaliana* and implications for the evolution of *Prochlorococcus* Species. *Plant Cell* **17**: 233-240.

Nakanishi, H., Nozue, H., Suzuki, K., Kaneko, Y., Taguchi, G., and Hayashida, N. (2005) Characterization of the *Arabidopsis thaliana* mutant pcb2 which accumulates divinyl chlorophylls. *Plant Cell Physiol* **46**: 467-473.

Orr, R.J.S., Stüken, A., Murray, S.A., and Jakobsen, K.S. (2013) Evolutionary acquisition and loss of saxitoxin biosynthesis in dinoflagellates: the second "core" gene - sxtG. *Appl Environ Microb* **79**: 2128-2136.

Palenik, B., Brahamsha, B., Larimer, F.W., Land, M., Hauser, L., Chain, P. et al. (2003) The genome of a motile marine *Synechococcus*. *Nature* **424**: 1037-1042.

Partensky, F., Hess, W., and Vaulot, D. (1999) *Prochlorococcus*, a marine photosynthetic prokaryote of global significance. *Microbiol Mol Biol Rev* **63**: 106-127.

Porra, R.J., Oster, U., and Scheer, H. (2011) Recent advances in chlorophyll and bacteriochlorophyll biosynthesis. In *Phytoplankton pigments: characterization, chemotaxonomy, and applications in oceanography*. Roy, S., Llewellyn, C.A., Egeland, E.S., and Johnsen, G. (eds). New York: Cambridge University Press, pp. 78-112.

Ralph, P.J., and Gademann, R. (2005) Rapid light curves: A powerful tool to assess photosynthetic activity. *Aquat Bot* **82**: 222-237.

Rebeiz, C.A., Ioannides, I.M., Kolossov, V., and Kopetz, K.J. (1999) Chloroplast biogenesis 80. Proposal of a unified multibranched chlorophyll *a*/*b* biosynthetic pathway. *Photosynthetica* **36**: 117-128.

Rourke, W.A., Murphy, C.J., Pitcher, G., Van de Riet, J.M., Garth Burns, B., Thomas, K.M., and Quilliam, M.A. (2008) Rapid postcolumn methodology for determination of paralytic shellfish toxins in shellfish tissue. *J AOAC Int* **91**: 589–597.

Roy, S., Llewellyn, C., Egeland, E., and Johnsen, G. (2011) *Phytoplankton pigments: characterization, chemotaxonomy, and applications in oceanography*. New York: Cambridge University Press.

Sakshaug, E., Bricaud, A., Dandonneau, Y., Falkowski, P.G., Kiefer, D.A., Legendre, L. et al. (1997) Parameters of photosynthesis: definitions, theory and interpretation of results. *J Plankton Res* **19**: 1637–1670.

Sakshaug, E., Bricaud, A., Dandonneau, Y., Falkowski, P.G., Kiefer, D.A., Legendre, L. et al. (1998) Parameters of photosynthesis: definitions, theory and interpretation of results (Erratum). *J Plankton Res* **20**: 603.

Salgado, P., Riobó, P., Rodríguez, F., Franco, J.M., and Bravo, I. (2015) Differences in the toxin profiles of *Alexandrium ostenfeldii* (Dinophyceae) strains isolated from different geographic origins: Evidence of paralytic toxin, spirolide, and gymnodimine. *Toxicon* **103**: 85-98.

Schreiber, U. (2004) Pulse-amplitude (PAM) fluorometry and saturation pulse method. In *Chlorophyll fluorescence: A Signature of Photosynthesis Advances in Photosynthesis and Respiration Series*. Papageorgiou, G.C. (ed). Dordrecht: Kluwer Academic Publishers, pp. 279-319.

Sleno, L., Chalmers, M., and Volmer, D. (2004) Structural study of spirolide marine toxins by mass spectrometry. Part II. Mass Spectrometric characterization of unknown spirolides

and related compounds in a cultured phytoplankton extract. *Anal Bioanal Chem* **378**: 977–986.

Stüken, A., Orr, R.J.S., Kellmann, R., Murray, S.A., Neilan, B.A., and Jakobsen, K.S. (2011) Discovery of nuclear-encoded genes for the neurotoxin saxitoxin in dinoflagellates. *PLoS One* **6**: e20096.

Tanaka, R., and Tanaka, A. (2007) Tetrapyrrole biosynthesis in higher plants. *Annu Rev Plant Biol* **58**: 321-346.

Tollefsbol, T. (2011) Epigenetics: the new science of genetics. In *Handbook of epigenetics: the new molecular and medical genetics*. Tollefsbol, T. (ed). USA: Academic Press, Elsevier, pp. 1-6.

Tomo, T., Akimoto, S., Ito, H., Tsuchiya, T., Fukuya, M., Tanaka, A., and Mimuro, M. (2009) Replacement of chlorophyll with di-vinyl chlorophyll in the antenna and reaction center complexes of the cyanobacterium *Synechocystis* sp. PCC 6803: Characterization of spectral and photochemical properties. *Biochim Biophys Acta* **1787**: 191-200.

Valle, K.C., Nymark, M., Aamot, I., Hancke, K., Winge, P., Andresen, K. et al. (2014) System responses to equal doses of photosynthetically usable radiation of blue, green, and red light in the marine diatom *Phaeodactylum tricornutum*. *PLoS One* **9**: e114211.

Wang, P., Gao, J., Wan, C., Zhang, F., Xu, Z., Huang, X. et al. (2010) Divinyl chlorophyll(ide) *a* can be converted to monovinyl chlorophyll(ide) *a* by a divinyl reductase in rice. *Plant Physiol* **153**: 994-1003.

Webb, W.L., Newton, M., and Starr, D. (1974) Carbon dioxide exchange of *Alnus rubra*: a mathematical model. *Oecologia* **17**: 281-291.

Wilhelm, C., Büchel, C., Fisahn, J., Goss, R., Jakob, T., LaRoche, J. et al. (2006) The regulation of carbon and nutrient assimilation in diatoms is significantly different from green algae, a putative consequence of secondary endosymbiosis. *Protist* **157**: 91-124.

Yacobi, Y.Z., Zohary, T., Kress, N., Hecht, A., Robarts, R.D., Waiser, M., and Wood, A.M. (1995) Chlorophyll distribution throughout the southeastern Mediterranean in relation to the physical structure of the water mass. *J Marine Syst* **6**: 179–190.

Zapata, M., and Garrido, J. (1991) Influence of injection conditions in reversed-phase high-performance liquid chromatography of chlorophylls and carotenoids. *Chromatographia* **31**: 589-594.

Zapata, M., Rodriguez, F., and Garrido, J.L. (2000) Separation of chlorophylls and carotenoids from marine phytoplankton: a new HPLC method using a reversed phase C8 column and pyridine-containing mobile phases. *Mar Ecol Prog Ser* **195**: 29-45.

Zapata, M., Garrido, J.-L., and Jeffrey, S.W. (2006) Chlorophyll *c* pigments: current status. In *Chlorophylls and Bacteriochlorophylls: Biochemistry, Biophysics, Functions and Applications*. Grimm, B., Porra, R.J., Rüdiger, W., and Scheer, H. (eds). Dordrecht: Springer, pp. 39-53.

Figure Captions

Fig. 1. (A) Chemical structure of chl *a* and DV-chl *a*. (B) HPLC chromatogram of AOTV-OS20 (DV-chl *a*-containing) and AOTV-OS16 (normal pigmented with trace levels of DV-chl *a*). Peak identification: 1) peridinin-like, 2) DV-Pchlide *a*, 3) chl c_2, 4) chl c_1, 5) peridinin, 6) peridinin-like, 7) peridinin-like, 8) diadinochrome, 9) diadinoxanthin, 10)

dinoxanthin, 11) diatoxanthin, 12) DV-chl *a*, 13) chl *a*, 14) pheophytin *a*, 15) β-carotene. (C) Absorbance spectrum (UV-VIS) and maxima in the blue region of DV-chl *a* (grey dotted line) and chl *a* (black solid line, normalized to DV-chl *a*) in HPLC eluent at room temperature.

Fig. 2. LC-MS results for DV-chl *a* in AOTV-OS20. Main fragment ions are indicated on the molecular structure of DV-chl *a*.

Fig. 3. (A) DV-chl *a*:chl *a* ratios in 3rd generation subclones (n=27) obtained from AOTV-C4-b28 clonal isolate.

Fig. 4. *In vivo* fluorescence of *A. ostenfeldii* isolates AOTV-OS16 (normal pigmented) and AOTV-OS20 (DV-chl *a*-containing) in LL (80 μmol photons · m^{-2} · s^{-1}) and HL (240 μmol photons · m^{-2} · s^{-1}) conditions and temperature (A) 15ºC and (B) 19ºC. Error bars represent standard deviations (n = 3).

Fig. 5. Rapid light curves obtained from PAM fluorometry in AOTV-OS16 (normal pigmented; solid lines and symbols) and AOTV-OS20 (DV-chl *a*-containing; dashed lines, open symbols) in LL and HL conditions, at 15 ºC and 19 ºC. Error bars represent standard deviations (n = 3).

Fig. 6. Operational quantum yield (Φ'_{PSII}) in AOTV-OS16 (normal pigmented; solid lines and symbols) and AOTV-OS20 (DV-chl *a*-containing; dashed lines, open symbols) in LL and HL conditions, and temperature (A) 15 ºC and (B) 19 ºC. Error bars represent standard deviations (n = 3).

Fig. 7. Photosynthesis-Irradiance curves measured from ^{14}C assimilation rates in AOTV-OS16 (normal pigmented; solid symbols) and AOTV-OS20 (DV-chl *a*-containing, open symbols).

Fig. 1

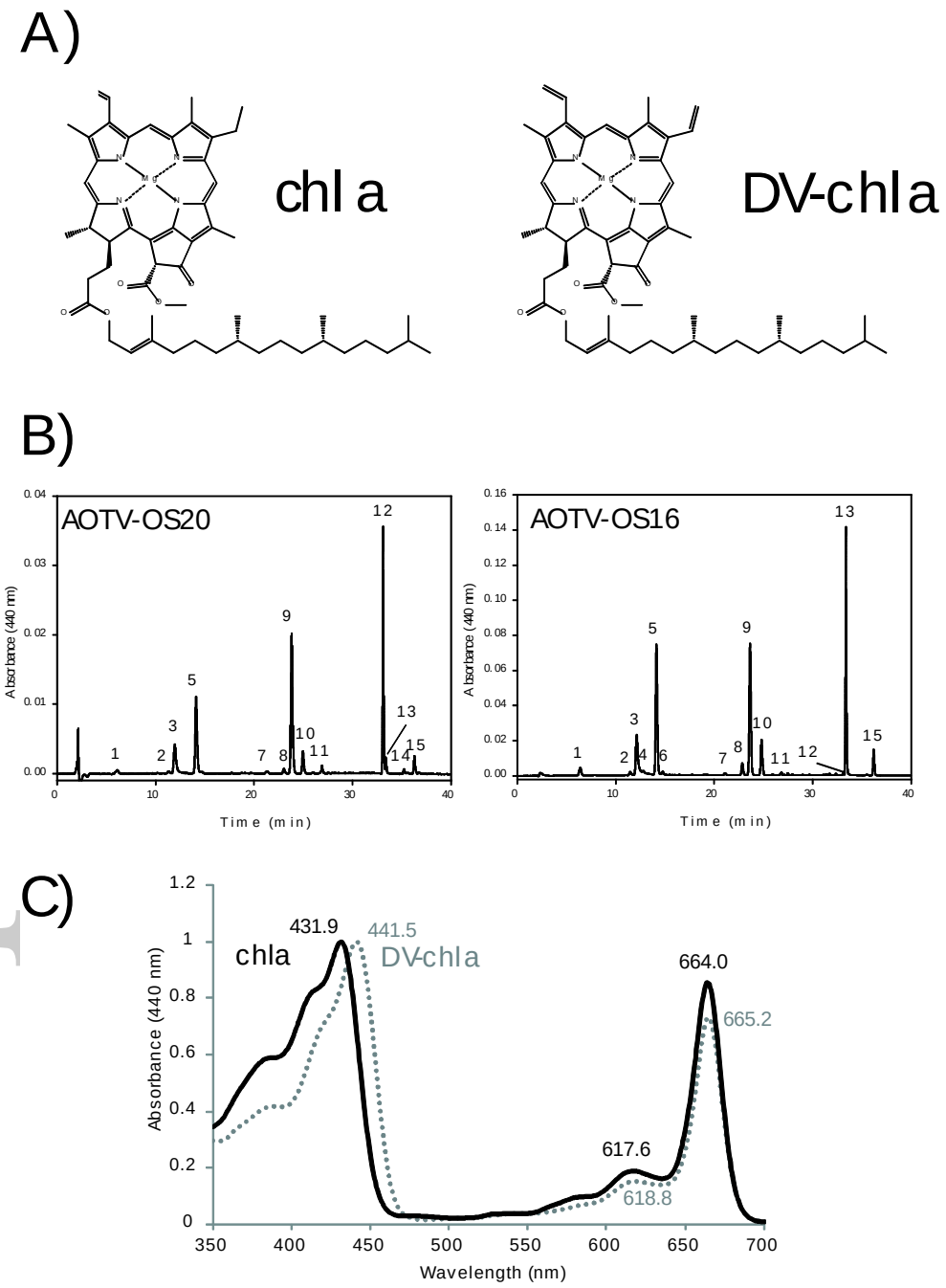

Fig. 2

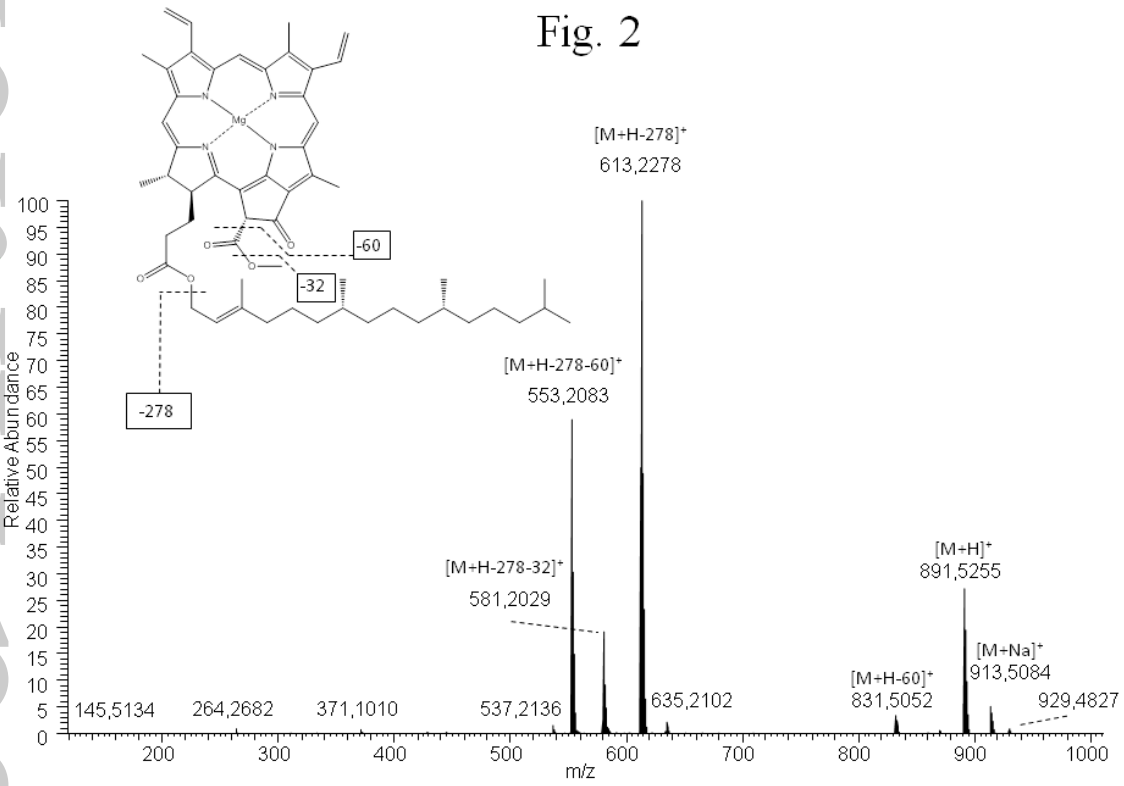

EMI_13042_F2

Fig. 3

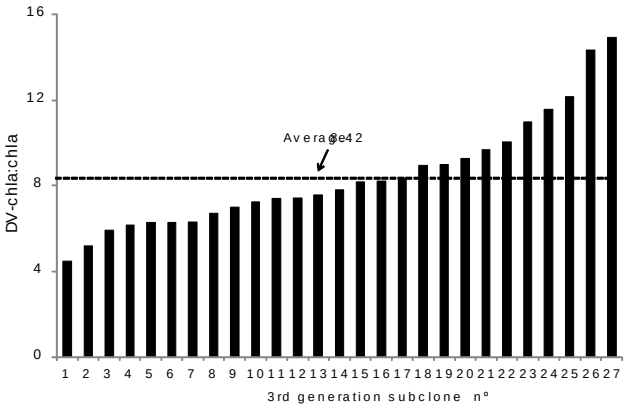

EMI_13042_F3

Fig. 4

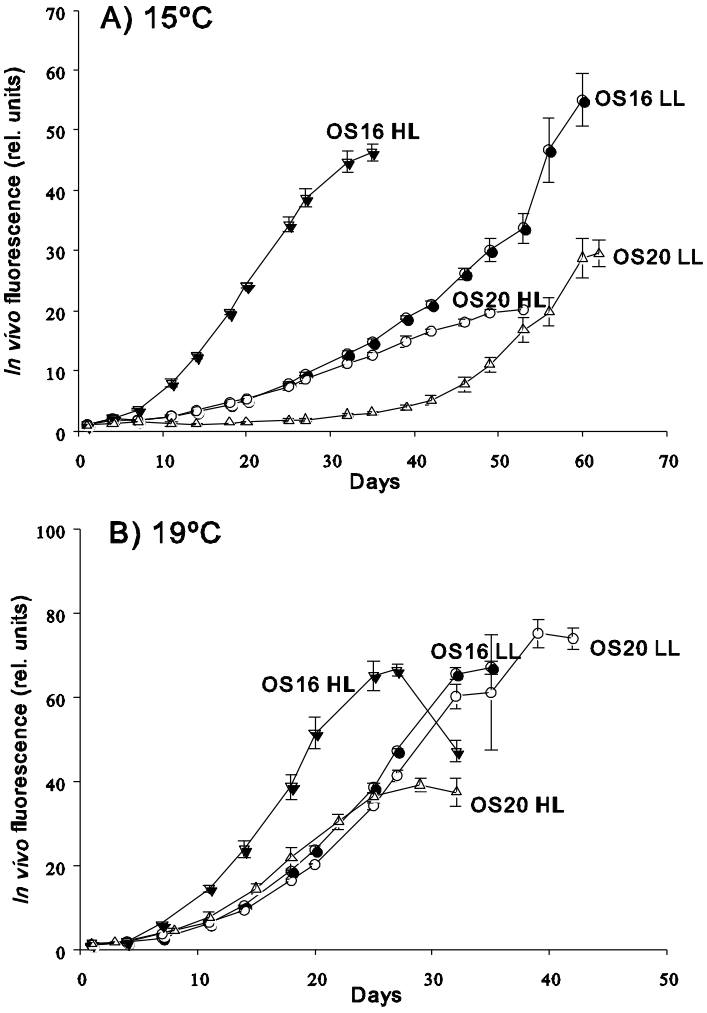

EMI_13042_F4

Fig. 5

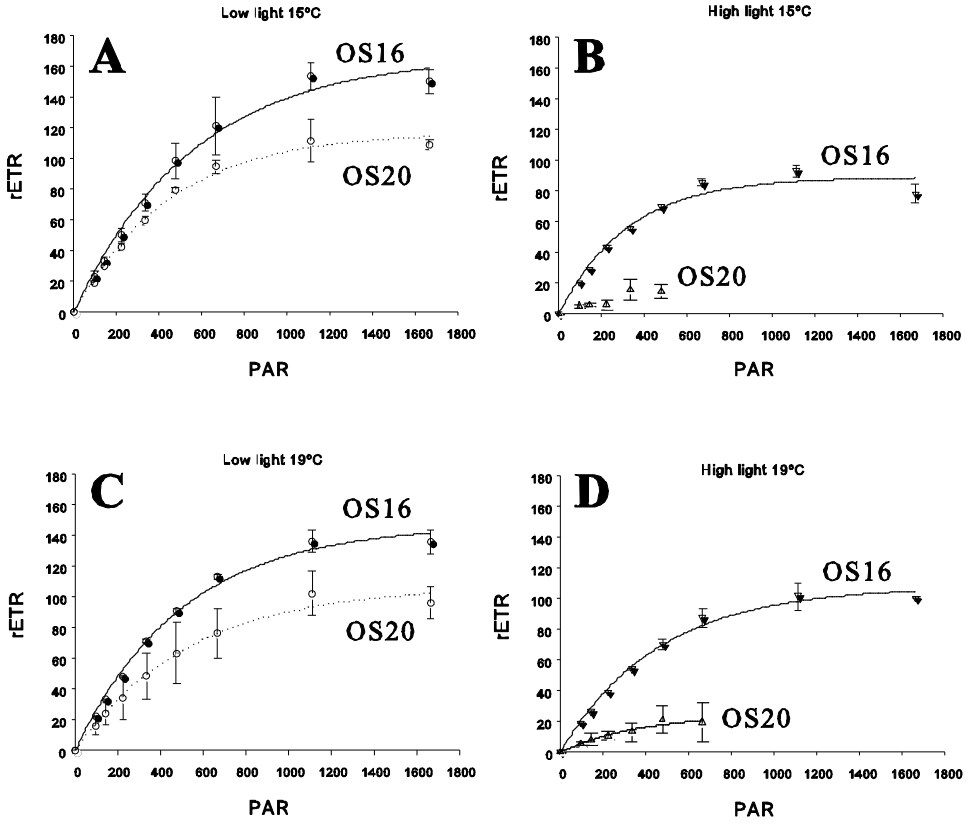

EMI_13042_F5

Fig. 6

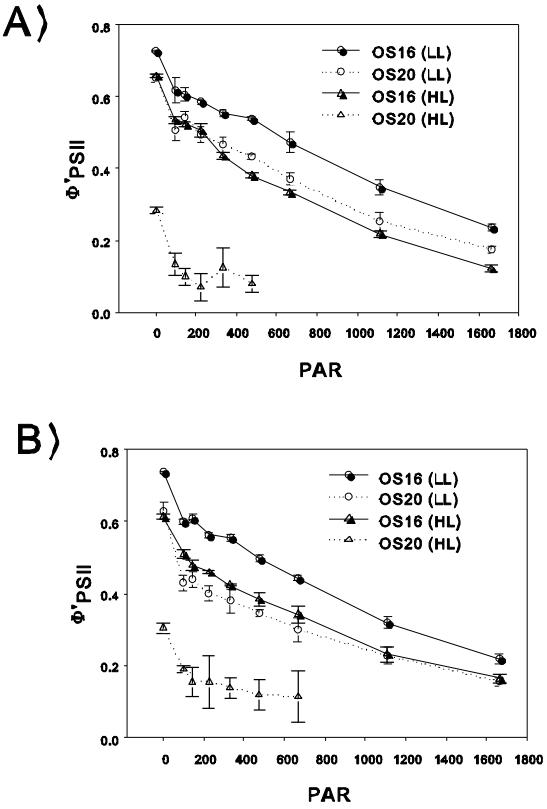

EMI_13042_F6

Fig. 7

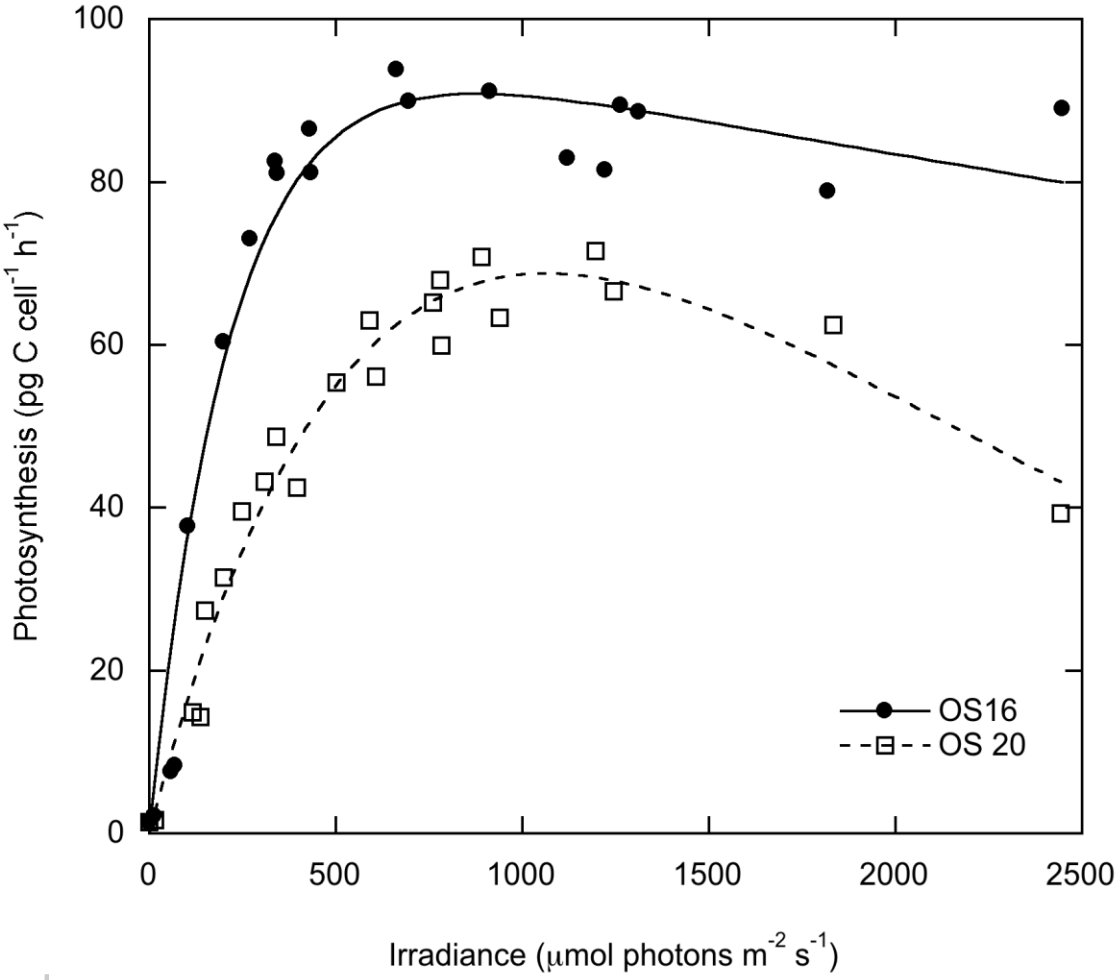

EMI_13042_F7

Table 1. Clonal strains of *Alexandrium ostenfeldii* (n=18) included in the present study and their pigment (molar) ratios. *AOTV-B3 and AOTV-C4 ratios are calculated as chl c_2/(DV-chl *a*+chl *a*) and peridinin (Per)/(DV-chl *a*+chl *a*).

Strains	chl c_2/*a**	chl c_1/c_2	Per/chl *a**	DV-chl *a*/chl *a*
AOTV-086	0.28	0.15	0.91	0.00
AOTV-081	0.32	0.10	0.91	0.00
AOTV-0814	0.28	0.26	1.01	0.00
AOTV-0811	0.34	0.12	1.09	0.00
AOTV-085	0.37	0.19	1.18	0.00
AOTV-0812	0.37	0.24	1.16	0.00
AOTV-0810	0.42	0.23	1.26	0.00
AOTV-0816	0.45	0.09	1.26	0.00
AOTV-0813	0.51	0.14	1.32	0.00
AOTV-0815	0.48	0.20	1.65	0.00
AOTV-088	0.54	0.12	1.68	0.00
AOTV-089	0.51	0.16	1.69	0.00
AOTV-082	0.50	0.19	1.72	0.00
AOTV-083	0.53	0.17	1.73	0.00
AOTV-A1	0.20	0.05	0.98	0.00
AOTV-A4	0.20	0.04	0.89	0.00
AOTV-B3	0.24	0.00	1.07	0.13
AOTV-C4	0.15	0.00	1.08	10.99

Table 2. Xanthophyll cycle de-epoxidation state (DES = Dt/(Dd+Dt)), DV-chl *a*:*a* ratios and photosynthetic parameters in AOTV-OS16 ("normal") and AOTV-OS20 (divinylic) from PAM-based RLC's in LL (80 μmol photons $m^{-2}s^{-1}$), HL (240 μmol photons $m^{-2}s^{-1}$), and temperature (15ºC and 19ºC) treatments. Values from extended RLC's (17 irradiances) are between parentheses; in the case of DV-strain these were calculated on AOTV-OS52. Significant differences in a given treatment between "normal" and divinylic strains (*P* values <0.005) are indicated with asterisks (n.d. for extended RLC's). [1]Includes minor amounts of chl c_1. [2]Values belong to 476 μmol photons $m^{-2}s^{-1}$.

Irradiance (μmol photons $m^{-2}s^{-1}$)		**Temperature (ºC)**			
		15		**19**	
		AOTV-OS16	**AOTV-OS20**	**AOTV-OS16**	**AOTV-OS20**
80	DES	0.05±0.00	0.03±0.00	0.07±0.01*	0.26±0.03*
	Per/Dd	9.88±0.05	9.51±0.05	8.68±0.25*	6.38±0.15*
	DV-chl *a*/chl *a*	<0.01*	2.98±0.15*	<0.01*	3.39±0.26*
	Σchl *c*:Σ*a*	0.12±0.05	0.16±0.01	0.27±0.01*	0.17±0.00*[1]
	Φ'_{PSII}	0.73±0.0	0.65±0.01	0.74±0.0	0.63±0.02
	$rETR_m$	167.2*	117.1*	146.9*	106.8*
	E_k	559* (366.2)	449* (466.4)	500 (612)	532 (363)
	α^*	0.299 (.316)	0.261 (.145)	0.293 (.336)	0.200 (.223)
	qP	0.36±0.01	0.29±0.02	0.34±0.02	0.31±0.02
	NPQ	0.28±0.02	0.33±0.02	0.37±0.03	0.35±0.05
240	DES	0.09±0.01	0.14±0.01	0.23±0.01*	0.52±0.02*
	Per/Dd	4.55±0.20*	2.33±0.01*	5.18±0.07*	3.82±0.16*
	DV-chl *a*/chl *a*	0.01±0.00*	11.36±0.68*	0.01±0.00*	5.03±0.59*
	Σchl *c*: Σ*a*	0.19±0.01*	0.08±0.01*	0.29±0.07*	0.11±0.02*
	Φ'_{PSII}	0.66±0.00*	0.28±0.01*	0.61±0.01*	0.30±0.01*
	$rETR_m$	88.7	--	107.6	--
	E_k	320 (363)	--	457 (559)	--
	α^*	0.277 (.245)	--	0.236 (.288)	--
	qP	0.64±0.02[2]	0.32±0.11[2]	0.66±0.03[2]	0.56±0.04[2]
	NPQ[1]	0.18±0.02[2]	0.05±0.03[2]	0.16±0.04[2]	0.07±0.03[2]

Table 3. Photosynthetic parameters (see methods) derived from ^{14}C assimilation rates and R^2 values for fitted *P-E* curves using Jassby and Platt (1976). Significant differences between strains (*P* values <0.005) are indicated with asterisks.

Strain	P^{14C}_m	α^{14C}	E_k	R^2
AOTV-OS16	67.1±14.5	0.243±0.060	291±4	0.98±0.01
AOTV-OS20	41.6±17.9	0.101±0.041	375±16	0.94±0.04

Table 4. Toxins composition (% of moles) in *A. ostenfeldii*; DV-strain AOTV-OS20 and normal chl *a* AOTV-OS16.

Strain	GTX3	GTX2	dcSTX	STX
AOTV-OS16	58.20	2.76	tr	39.04
AOTV-OS20	47.16	3.45	-	49.39

Table 5. Definitions of the productivity, photosynthetic, and bio-optical parameters used in the text.

Φ'_{PSII}	Operational quantum yield for PSII charge separation (eq. 1, mol electrons · [mol quanta]$^{-1}$)
$\alpha^{*\,14C}$	Maximum light utilization coefficient (derived from PAM fluorescence, or normalized to carbon in eq. 7, ^{14}C · [mg TOC]$^{-1}$ ·h^{-1} [µmol · m^{-2} · s^{-1}]$^{-1}$)
P^{14C}	Photosynthetic rate per unit of chlorophyll biomass (mg C [mg Chl *a*]$^{-1}$ h^{-1})
P_m^{14C}	Maximum photosynthetic rate normalized to chlorophyll biomass (mg C [mg Chl *a*]$^{-1}$ h^{-1})
E_k	Light saturation index (µmol photons · m^{-2} · s^{-1})